ELSEVIER

Carbohydrate Research 291 (1996) 141–154

CARBOHYDRATE RESEARCH

Structural analysis of acetylated hemicellulose polysaccharides from fibre flax (*Linum usitatissimum* L.)

Johanna M. van Hazendonk *, Erna J.M. Reinerink, Pieter de Waard, Jan E.G. van Dam

ATO-DLO Agrotechnological Research Institute, P.O. Box 17, NL-6700 AA Wageningen, The Netherlands

Received 13 November 1995; accepted 10 June 1996

Abstract

Hemicellulose polysaccharides were sequentially extracted from defatted and depectinized flax bast fibres with Me_2SO (20 °C), hot water (100 °C), aq 5% NaOH (20 °C), and aq 17.5% NaOH (20 °C). The ethanol-precipitated Me_2SO extract was fractionated by size-exclusion chromatography, and the two main fractions (fraction II and III), covering 85% of the total, were analyzed by HPLC for constituting monosaccharides and acetyl content, and by NMR spectroscopy (^1H, ^{13}C and 2D-heteronuclear proton detected multiple-bond coherence (HMBC)). Fraction II contained a linear β-(1 → 4)-linked xylan, *O*-acetylated on C-2 and C-3 with an acetylation degree of 0.5. Fraction III was enriched in Man and Glc residues. NMR spectral data gave evidence for the presence of a linear β-(1 → 4)-linked glucomannan, *O*-acetylated on C-2 and C-3 of Man with an acetylation degree of 0.5 (based on Man). HPLC analysis and ^1H and ^{13}C NMR spectral data showed that the ethanol-precipitated hot-water extract consists of an *O*-acetylated rhamnogalacturonan I (RG-I) type structure. HPLC analysis of neutral monosaccharides indicates that the alkaline extracts are composed of glucomannan, xylan, and RG-I, having similar structures as those found in the Me_2SO and hot-water extracts. © 1996 Elsevier Science Ltd.

Keywords: Flax; Hemicellulose; Glucomannan; Xylan; *O*-Acetylation

1. Introduction

Bast fibres from fibre flax (*Linum usitatissimum* L.) are used in the textile industry for the production of linen yarns and fabrics. Traditionally, the bast fibre bundles are

* Corresponding author.

PII S0008-6215(96)00160-7

separated from the plant by retting, which is a microbial degradation of pectins and other binding components. The resulting fibre bundles are composed of several individual fibres, which are single thick-walled cells. Chemically, retted flax fibres contain, depending on the retting degree, 65–80% cellulose, 12–16% hemicellulose polysaccharides, 2–5% pectic materials, 2–4% lignin, and 2–5% waxes, minerals and proteins [1].

The non-cellulosic polysaccharides (pectins and hemicellulose) make up approximately 20% of the flax bast fibre and significantly contribute to fibre properties such as water absorbancy, swelling, elasticity and (wet) strength. Understanding the composition, structure, and location of these polysaccharides is important to be able to explain fibre properties and thus to control fibre quality during processing. Moreover, fibre modifications for improvement of properties can be performed more effectively if fibre composition and structure are known.

Since knowledge of the pectic structure is important to be able to control the retting process and thus fibre quality, these components have been extensively investigated [2–5]. The composition and structure of the hemicellulose polysaccharides is less clear. McDougall [6] showed that flax hemicellulose contains a β-(1 $\rightarrow$ 4)-linked glucomannan, and found evidence for the presence of xylan and some xyloglucan. However, these hemicellulose fractions were extracted by alkaline solutions. Under these conditions, *O*-acetyl groups are removed, which precludes the possibility of showing their presence [7]. The *O*-acetyl groups can strongly influence polysaccharide properties such as solubility, water sorption, swelling and hydrophobicity, and therewith fibre properties. Morvan et al. [3] extracted a hemicellulose polysaccharide enriched in Gal and Glc by boiling with aq 6% NaOH. The combination of alkali and high temperature will, however, cause extensive alkaline degradation.

The aim of this study is to establish the structure of *O*-acetylated hemicellulose polysaccharides from fibre flax. In order to isolate *O*-acetylated polysaccharides, an extraction procedure developed for the isolation of *O*-acetylated wood polysaccharides was used [8].

2. Experimental

Materials.—Water-retted and scutched flax fibres (variety Belinka) were ground in a cutting mill (Retsch) to pass a 0.5 mm screen. The milled fibres were defatted by refluxing with aq 95% EtOH for 6 h, then air-dried. Subsequently, pectins were extracted in aq 1% ammonium oxalate (pH 5.0) for 2 $\times$ 2 h at 80 °C. All chemicals used were of analytical grade. Distilled water was used throughout unless stated otherwise.

Extraction of hemicellulose polysaccharides.—The following extractions were performed sequentially on 20 g of defatted and depectinized flax fibre: (1) Me_2SO (10 mL/g fibres), 2 $\times$ 16 h, 20 °C; (2) water (22.5 mL/g fibres), 2 $\times$ 30 min, 100 °C; (3) aq 5% NaOH (50 mL/g fibres), 2 h, 20 °C; (4) aq 17.5% NaOH and 0.1 M $NaBH_4$ (50 mL/g fibres), 2 h, 20 °C. The Me_2SO extracts were combined and EtOH was added until a concentration of 75% EtOH was reached, in order to precipitate the hemicellulose polysaccharides. The water extracts were combined and concentrated in vacuo to a final volume of 100 mL. Hemicellulose polysaccharides were precipitated by adding 400 mL

EtOH. The alkaline extracts were neutralized with glacial acetic acid and precipitated in 75% EtOH. Precipitates were recovered by centrifugation (15,000 × *g*; 40 min), washed with EtOH, dissolved in water, and lyophilized.

Size-exclusion chromatography of Me_2SO extract.—The lyophilized Me_2SO extract (300 mg) was dissolved in milliQ water (10 mg/mL), and fractionated on a Sephacryl S400 HR column (60 × 0.16 cm, Pharmacia) eluted with milliQ water (60 mL/h), and monitored with a refractive index detector (Pharmacia). The column was calibrated with dextran standards (Pharmacia) from 10 kDa up to 2000 kDa, giving a good linearity ($R^2 = 98.3$) between log *M* and exclusion volume. The eluent was collected in four fractions according to the four major elution peaks. The fractions of several runs were pooled and lyophilized.

Analytical methods.—For the monosaccharide analysis, total and fractionated extracts were sequentially hydrolyzed in 12 M H_2SO_4 (1 h, 30 °C) and 1 M H_2SO_4 (3 h, 100 °C). High-performance anion-exchange chromatography (HPAEC) was carried out on a CarboPac PA-1 column (4 × 250 mm, Dionex) using pulsed amperometric detection (PAD, Dionex) [9]. For neutral monosaccharide analysis the column was eluted at 38 °C with a gradient of 15 mM NaOH to milliQ water in 0.1 min, followed by milliQ water for 40 min at a flow rate of 0.8 mL/min. For uronic acid determinations the column was eluted at 30 °C with a gradient of 0–300 mM NaOAc at a flow rate of 0.8 mL/min. *O*-Acetyl groups were released in 0.6 M NaOH in 1:1 water–isopropanol, and the *O*-acetyl content was determined by HPLC [10].

NMR analysis.—The structure of the compounds present in the two major Me_2SO fractions and the unfractionated water extract were determined by NMR spectroscopy. Samples were dissolved in D_2O (99.96 at% D). ^1H and ^{13}C NMR spectra were recorded on a Bruker AMX 500 or on a Bruker AMX 400 wb NMR spectrometer at probe temperatures of 27 or 70 °C. The *O*-acetyl groups in the two major Me_2SO fractions were localized by 2D-heteronuclear proton-detected multiple-bond coherence (HMBC) NMR spectroscopy [11]. HMBC spectra were recorded on a Bruker AMX 500 NMR spectrometer using a probe temperature of 70 °C. For fraction II 512 experiments of 2048 data points, consisting of 320 scans per t_1 value, and for fraction III 1024 experiments of 2048 data points, consisting of 160 scans per t_1 value, were recorded. The time domain data were multiplied with a phase-shifted sine-square window. Phase-sensitive Fourier transformation, resulting in data sets of 1024 × 1024 complex points, was followed by an absolute-value calculation in the t_2 direction. Chemical shifts are expressed in ppm relative to internal acetone (^1H, δ 2.225; ^{13}C, δ 31.55).

3. Results and discussion

Extractions.—The yields of the sequential extractions of the flax fibres are shown in Table 1. All values are calculated on basis of the unextracted starting material. These results show that flax fibres contain approximately 3.6% fatty substances (EtOH extract), 6.5% pectic material (ammonium oxalate extract), 14.6% hemicellulose polysaccharides (Me_2SO, hot-water, and NaOH extracts), and 75.3% cellulose.

Table 1
Yields of subsequent extractions of flax fibres

Solvent	Temperature (°C)	Yield (%)
95% Ethanol	b.p. [a]	3.6 [b]
Aq 1% ammonium oxalate	80	6.5 [c]
Me_2SO	20	2.1 [b]
H_2O	100	0.7 [b]
Aq 5% NaOH	20	5.5 [c]
Aq 17.5% NaOH	20	6.3 [c]
Total		24.7

[a] b.p. = boiling point.
[b] Based on extract recovery.
[c] Based on weight loss.

Me_2SO and water are expected to extract hemicellulose polysaccharides without degradation, in contrast to alkaline extractions which will cause de-*O*-acetylation. For this reason structural analysis is only performed on the Me_2SO- and hot-water-soluble hemicellulose polysaccharides. Subsequent alkaline extractions are performed to determine the total hemicellulose content.

Me_2SO extract.—97.3% of the lyophilized Me_2SO extract could be dissolved in water and was fractionated on Sephacryl S400 giving rise to four peaks, denoted I–IV (Fig. 1). The fractions I, II, III and IV account for 7, 21, 64 and 5% of the weight of the Me_2SO extract, respectively, and 3% of the extract is insoluble. The two main fractions (fraction II and III) together account for 85% of the total Me_2SO extract and were the

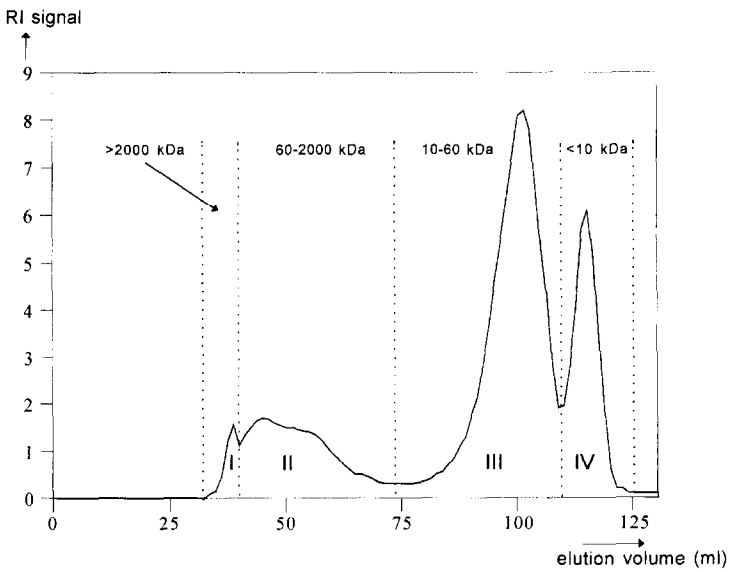

Fig. 1. Elution profile of Me_2SO extract.

Table 2
Monosaccharide composition (mol%), *O*-acetyl content and total carbohydrate content of the hemicellulose-containing fractions and extracts

Monosaccharide	Extracts						
	Me_2SO				Water	Aq 5% NaOH	Aq 17.5% NaOH
	I	II	III	IV			
Rha	2	1	0	< 1	11	2	1
Ara	13	1	< 1	3	12	1	1
Gal	35	2	3	2	54	8	5
Glc	16	4	33	25	3	33	35
Xyl	23	88	14	36	4	11	4
Man	3	2	49	30	1	42	53
GalA	6	2	< 1	3	14	2	1
GlcA	1	< 1	< 1	< 1	< 1	< 1	0
OAc	18	40	24	13	31	n.d. [a]	n.d. [a]
Total carbohydrate	41%	71%	81%	66%	47%	66%	48%

[a] n.d. = not determined.

only fractions analyzed in detail. The molecular masses (see Fig. 1) are estimations since they are determined by calibration with linear dextrans, probably not possessing the same hydrodynamic volume as the hemicellulose polysaccharides. The monosaccharide composition of the Me_2SO fractions is shown in Table 2.

Fraction II.—The Me_2SO fraction II is enriched in Xyl (Table 2). It has a molecular mass of 60–2000 kDa, which corresponds to a degree of polymerization of 450–1500.

The ^1H and HMBC spectra of fraction II are shown in Fig. 2. The ^1H and ^{13}C NMR chemical shifts are presented in Table 3. The ^1H and ^{13}C signals of $\rightarrow$ 4)-β-D-Xyl*p*-(1 $\rightarrow$ are in accordance with literature values [12–15]. The ^{13}C signals in the regions of 23 and 176 ppm can be assigned to CH_3 and CO, respectively, of an *O*-acetyl group, indicating that the xylan is *O*-acetylated. HMBC spectroscopy was used to assign the *O*-acetylated Xyl residues.

Since no decoupling is applied during acquisition of the HMBC spectrum, the single-bond cross-peaks can easily be recognized from their large proton–carbon coupling constants (proton–carbon pairs indicating single-bond cross-peaks have identical numbers in Fig. 2). Due to the low resolution of the 2D spectrum, the small couplings of multiple-bond correlations (usually two- and three-bond couplings between protons and carbons) remain within the line width.

The cross-peak at ^1H, δ 4.94; ^{13}C, δ 175 in Fig. 2, is assigned as a multiple-bond correlation of the C=O carbon of an *O*-acetyl group with the proton attached to the *O*-acetylated carbon. On a vertical line starting from this cross-peak one single-bond and two multiple-bond correlations with the proton attached to the *O*-acetylated carbon are found. Assignment of the carbons involved in these correlations is possible by comparing the carbon chemical shifts found for these cross-peaks with those of non-*O*-acetylated Xyl residues (Table 3). It can be calculated that *O*-acetylation results in a downfield shift for the *O*-acetylated carbon and an upfield shift for its two neighbouring carbons

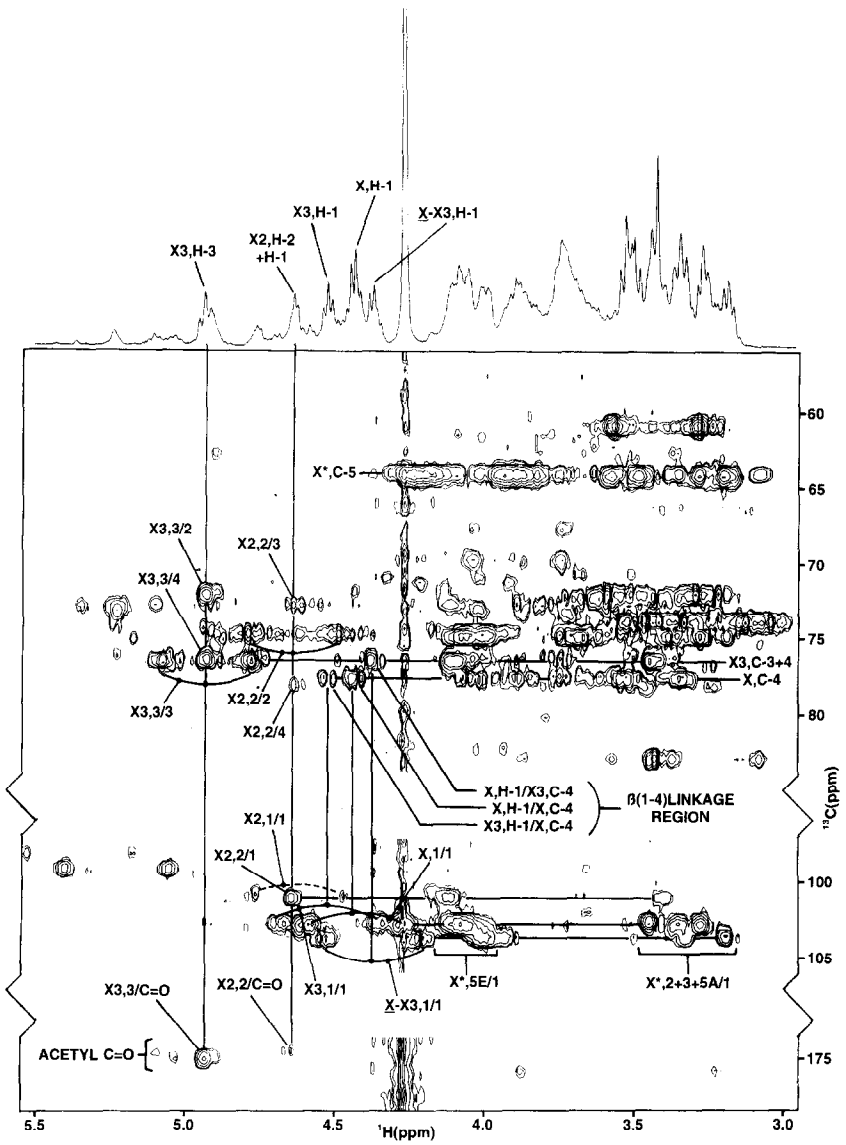

Fig. 2. ^{1}H and HMBC NMR spectra of fraction II. The letters and numbers in the spectra refer to the corresponding residues and the H- and/or C-atoms, with the following encoding: X, non-acetylated Xyl; X2, 2-*O*-acetylated Xyl; X3, 3-*O*-acetylated Xyl; X–X3, the signals of a non-acetylated Xyl which is linked to a 3-*O*-acetylated Xyl; X*, any Xyl; 5A, axial H-5; 5E, equatorial H-5. Cross-peaks resulting from single or multiple-bond coherences are indicated with two numbers, the first one referring to the proton and the second to the C-atom involved in the coherence. For example: X3,3/4 indicates a coherence between H-3 and C-4 of a 3-*O*-acetylated Xyl residue. Cross-peaks of single-bond coherences, indicated by identical proton and carbon numbers, are split by the large single-bond proton–carbon couplings.

Table 3
^{1}H and ^{13}C chemical shifts in ppm for the constituent monomers of fraction II

Residue	^{1}H chemical shifts [a]			^{13}C chemical shifts [a]				
	H-1	H-2	H-3	C-1	C-2	C-3	C-4	C-5
X	4.44	3.28	3.54	102.96	73.99	74.94	77.64	64.3
X–X3	4.38	3.20	3.54	103.92	73.99	74.94	77.64	64.3
X3	4.53	3.28	4.94	102.71	72.19	76.77	76.52	64.3
X2	4.64	4.64	3.51	101.13	74.8	72.73	n.d. [b]	64.3

[a] ^{1}H chemical shifts are measured at 343 K and at 500 MHz. ^{13}C chemical shifts are measured at 300 K and at 100 MHz. The following encoding is used: X, non-acetylated Xyl; X2, 2-*O*-acetylated Xyl; X3, 3-*O*-acetylated Xyl; X–X3, the signals of a non-acetylated Xyl which is linked to a 3-*O*-acetylated Xyl. The following chemical shifts are found for the acetyl carbon signals: X2 C=O, 174.48; X2 CH_3, 21.66; X3 C=O, 175.00; X3 CH_3, 21.89; and for the acetyl proton signals: X2 CH_3, 2.07; X3 CH_3, 2.12.
[b] n.d. = not detected.

[16]. The assignment shown in Fig. 2 with the *O*-acetyl group at C-3 is the only possible assignment which fits this pattern: C-3 is shifted downfield and both C-2 and C-4 are shifted upfield. Starting from the C=O region at 175 ppm, also signals of a small amount of 2-*O*-acetylated Xyl can be identified in Fig. 2 in a similar way as has been discussed for 3-*O*-acetylated Xyl.

In the HMBC spectrum cross-peaks are present over the glycosidic linkage between H-1 and C-4. Three cross-peaks are identified in the β-(1 → 4)-linkage region. Starting from C-4 of non-*O*-acetylated Xyl at 77.64 ppm the cross-peak at 4.44 ppm is assigned to H-1 of non-*O*-acetylated Xyl and the cross-peak at 4.53 ppm is assigned to H-1 of 3-*O*-acetylated Xyl. Starting from C-4 of 3-*O*-acetylated Xyl at 76.52 ppm, only the cross-peak with a non-*O*-acetylated Xyl H-1 at 4.38 ppm is assigned. The downfield shifts for H-1 and H-3 of 3-*O*-acetylated Xyl and the upfield shift for the H-1 of the Xyl residue β-(1 → 4)-linked to 3-*O*-acetylated Xyl are in accordance with the results found for fraction III.

Splitting of signals in the proton and carbon spectra indicates that various possible combinations of sugar residues, resulting from the random distribution of *O*-acetyl groups, probably are present. A detailed assignment of these combinations, as is given for fraction III, is not possible here, since not enough information is available in the spectrum, especially in the β-(1 → 4)-linkage region. For assignment of minor signals, such as at 5.24 ppm, there is also not enough information available.

From the NMR and HPLC analyses, it can be concluded that fraction II contains a β-(1 → 4)-linked xylan, *O*-acetylated on the C-2 and C-3 positions of the Xyl residues. The degree of acetylation of the Xyl residues, as determined by HPLC, is 0.5 (see Table 2). The intensities of the H-1 and H-3 signals of 3-*O*-acetylated Xyl and of the H-1 and H-2 signals of 2-*O*-acetylated Xyl indicate that approximately 75% of the *O*-acetyl groups is situated on C-3 of Xyl and 25% on C-2. In contrast to most cell wall xylans [7,17], this xylan hardly contains any GlcA.

Fraction III.—The Me_2SO fraction III is enriched in Man and Glc and, to a lesser extent, Xyl (Table 2), suggesting it to consist of glucomannan and some xylan

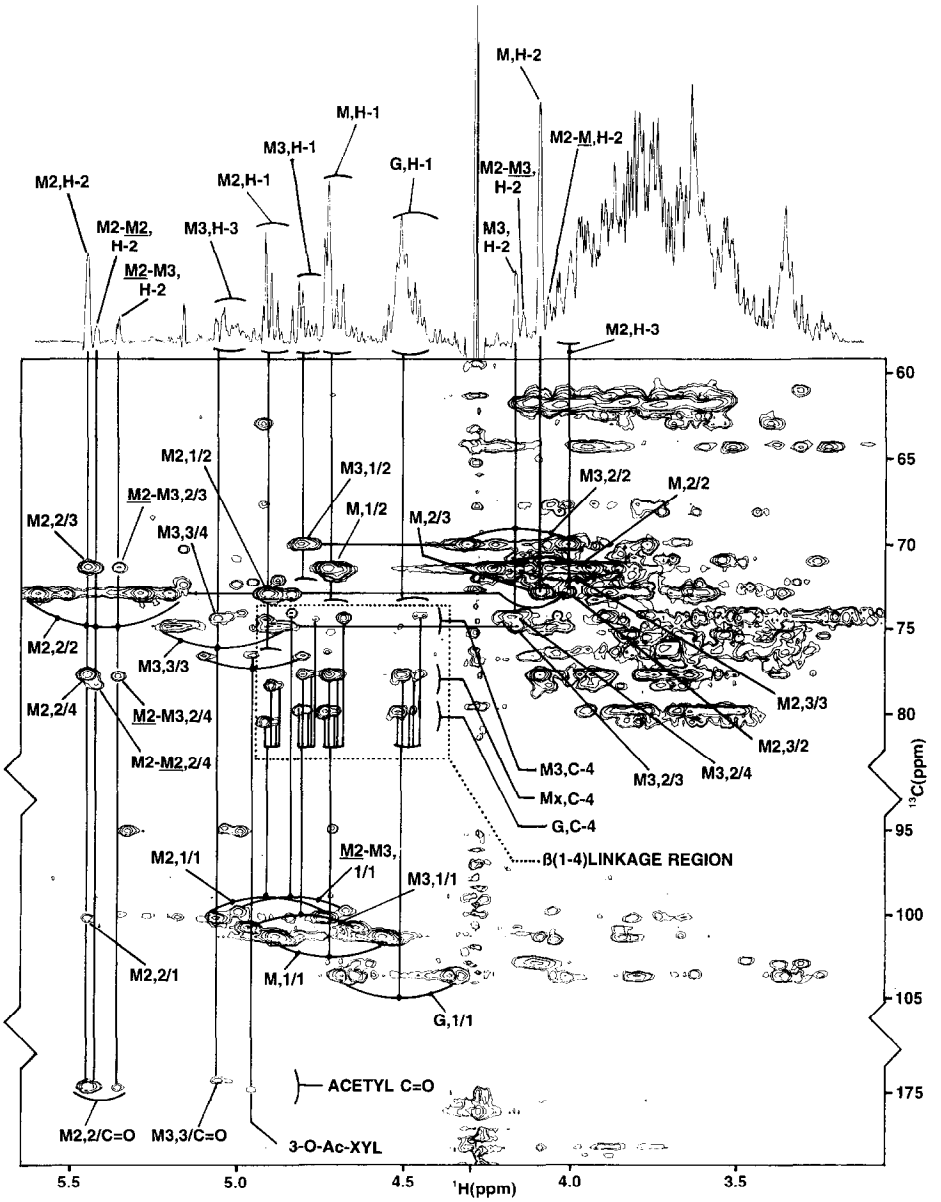

Fig. 3. ^{1}H and HMBC NMR spectra of fraction III. The letters and numbers in the spectra refer to the corresponding residues and the H- and/or C-atoms, with the following encoding: G, Glc; M, non-acetylated Man; M2, 2-*O*-acetylated Man; M3, 3-*O*-acetylated Man; Mx, M or M2; M2–M3 (as an example), the signals of a 2-*O*-acetylated Man which is linked to a 3-*O*-acetylated Man. Cross-peaks resulting from single or multiple-bond coherences are indicated with two numbers, the first one referring to the proton and the second to the C-atom involved in the coherence. For example: M3,3/4 indicates a coherence between H-3 and C-4 of a 3-*O*-acetylated Man residue. Cross-peaks of single-bond coherences, indicated by identical proton and carbon numbers, are split by the large single-bond proton–carbon couplings.

Table 4
^{1}H and ^{13}C chemical shifts in ppm for the constituent monomers of fraction III

Residue	^{1}H chemical shifts [a]			^{13}C chemical shifts [a]			
	H-1	H-2	H-3	C-1	C-2	C-3	C-4
S–M–Mx	4.714	4.080	n.d. [b]	101.42	71.3	72.8	77.7
M2–M–Mx	4.671	4.053	n.d.	101.42	71.3	72.8	78.7
S–M–G	4.726	4.080	n.d.	101.29	71.3	72.8	77.7
M2–M–G	4.690	4.053	n.d.	101.29	71.3	72.8	78.7
S–M–M3	4.671	3.990	n.d.	101.3	71.3	72.8	77.7
M2–M–M3	4.632	n.d.	n.d.	101.3	71.3	72.8	78.7
S–M2–Mx	4.888	5.435	4.01	100.34	72.8	71.3	77.7
M2–M2–Mx	4.857	5.409	4.01	100.34	72.8	71.3	78.7
S–M2–G	4.904	5.435	4.01	100.2	72.8	71.3	77.7
M2–M2–G	4.869	5.409	4.01	100.2	72.8	71.3	78.7
S–M2–M3	4.825	5.346	4.01	99.90	72.8	71.3	77.7
M2–M2–M3	4.78	n.d.	4.01	99.90	72.8	71.3	78.7
S–M3–Mx	4.793	4.153	5.043	100.89	70.0	74.7	74.2
M2–M3–Mx	4.766	4.128	4.98	100.89	70.0	74.7	74
S–M3–G	4.805	4.153	5.043	100.73	70.0	74.7	74.2
M2–M3–G	4.777	4.128	4.98	100.73	70.0	74.7	74
S–M3–M3	4.753	4.209	5.0	100.8	70.0	74.7	74.2
M2–M3–M3	4.71	n.d.	5.0	100.8	70.0	74.7	74
S–G–Mx	4.489	n.d.	n.d.	103.79	74.2	n.d.	79.7
M2–G–Mx	4.449	n.d.	n.d.	103.79	74.2	n.d.	80.53
S–G–G	4.503	n.d.	n.d.	103.68	74.2	n.d.	79.7
M2–G–G	4.464	n.d.	n.d.	103.68	74.2	n.d.	80.53
S–G–M3	4.437	n.d.	n.d.	103.7	74.2	n.d.	79.7
M2–G–M3	4.389	n.d.	n.d.	103.7	74.2	n.d.	80.53

[a] ^{1}H chemical shifts are measured at 343 K and at 500 MHz. ^{13}C chemical shifts are measured at 300 K and at 100 MHz. The following encoding is used: G, Glc; M, non-acetylated Man; M2, 2-*O*-acetylated Man; M3, 3-*O*-acetylated Man; Mx, M or M2; S, any monosaccharide, except M2. The values are given for the signals of the underlined residue. For example: M2–M3–G refers to the values for M3 within the sequence M2-β-(1 → 4)-M3-β-(1 → 4)-G. The following chemical shifts are found for the acetyl carbon signals: M2 C=O, 174.72; M2 CH_3, 21.86; M3 C=O, 174.3; M3 CH_3, 21.61; and for the acetyl proton signals: M2 CH_3, 2.16; M3 CH_3, 2.13.
[b] n.d. = not detected.

polysaccharides. The molecular mass of this fraction ranges from 10 to 60 kDa, which means a degree of polymerization of 60–400.

The 500 MHz ^{1}H and HMBC spectra of fraction III are shown in Fig. 3. The ^{1}H and ^{13}C chemical shifts are listed in Table 4. The main signals in the ^{13}C spectrum can be assigned to the C-atoms of → 4)-β-D-Man*p*-(1 → and → 4)-β-D-Glc*p*-(1 → [18–21], thereby giving evidence of the presence of a β-(1 → 4)-linked glucomannan. The ^{13}C signals in the regions of 22 and 175 ppm can be assigned to CH_3 and CO, respectively, of an *O*-acetyl group, indicating that the glucomannan is *O*-acetylated. The main signals of protons attached to *O*-acetylated C-atoms are found around 5.4 ppm, and are, based on their coupling patterns in the 1D spectrum, assigned to Man H-2. In the HMBC

spectrum (Fig. 3), on vertical lines starting from these signals, cross-peaks with Man C-1,2,3,4 can be identified, besides cross-peaks with acetyl C=O. Although C-2 of 2-*O*-acetylated Man is coinciding with C-3 of non-*O*-acetylated Man and C-3 of 2-*O*-acetylated Man is coinciding with C-2 of non-*O*-acetylated Man, correct assignment pathways, using the advantage of the mentioned difference between single-bond and multiple-bond cross-peaks, can be identified in Fig. 3. Due to 2-*O*-acetylation the Man H-1, H-2, and C-2 signals are shifted downfield with $\Delta\delta$ 0.17, 1.36, and 1.5, respectively. The Man C-1 and C-3 signals are shifted upfield with $\Delta\delta$ 1.3 and 1.5, respectively.

In the same way, the signals around 5.0 ppm can be assigned to H-3 of 3-*O*-acetylated Man. Similar to the results for 2-*O*-acetylated Man, H-2, H-3, and C-3 of 3-*O*-acetylated Man are shifted downfield, whereas C-2 and C-4 are shifted upfield. This is in accordance with observations by Jansson et al. [22], who determined chemical shifts due to mono-*O*-acetylation for α- and β-D-gluco- and galacto-pyranosides and found shifts from 1.1 to 1.4 ppm for 2-*O*-acetylated H-2 and 0.18–0.23 ppm for 3-*O*-acetylated H-2, respectively. The *O*-acetyl groups also induce small but distinct chemical shift effects further away in the polymer. The H-1 of 3-*O*-acetyl-Man is shifted downfield and both H-1 and H-2 of the sugar β-(1 → 4)-linked to 3-*O*-acetylated Man are shifted upfield. A 2-*O*-acetylated Man has influence on the residue it is attached to: C-4 is shifted downfield, and for H-1 a small upfield shift is observed.

Results from Goldberg et al. [21] and Westerlund et al. [23] show that the chemical shifts of 4-linked glucopyranosyl and mannopyranosyl residues are differently affected by neighbouring monosaccharide residues. Since the 2-*O*- and 3-*O*-acetyl groups apparently are randomly distributed, there is a large number of possible monosaccharide combinations resulting in a large number of cross-peaks in the β-(1 → 4)-linkage region (Fig. 4). Cross-peaks of the H-1 signals of 2-*O*-acetylated Man, 3-*O*-acetylated Man, non-*O*-acetylated Man, and Glc with C-4 of Glc are identified, indicating β-(1 → 4)-linkages of all possible residues with Glc. These cross-peaks are not all on a single line of Glc C-4 at 79.7 ppm, since Glc C-4 is shifted upfield to 80.53 ppm, if a 2-*O*-acetylated Man is attached to Glc. The attachment of 2-*O*-acetylated Man to the monosaccharide β-(1 → 4)-linked to Glc results in an upfield shift of H-1, resulting in doubling of each cross-peak. All possible β-(1 → 4)-linkages with Glc results in a pattern of cross-peaks. This pattern is also found for β-(1 → 4)-linkages with 2-*O*- or non-acetylated Man (denoted in Fig. 4 as Mx), with C-4 resonating at 78 ppm for both residues. Finally, a similar pattern of cross-peaks is also found for β-(1 → 4)-linkages with 3-*O*-acetylated Man, with C-4 resonating at 74 ppm. The carbon chemical shift belonging to the cross-peak of 2-*O*-acetylated Man H-1 with 3-*O*-acetylated Man C-4 deviates from this pattern. This can probably be ascribed to conformational changes due to interaction of the two neighbouring acetyl groups.

The remaining signals can be attributed to → 4)-β-D-Xyl*p*-(1 → , probably a contamination from fraction II.

The HPLC and NMR analyses show that fraction III consists of a β-(1 → 4)-linked glucomannan with a Man/Glc ratio of 1.5, *O*-acetylated on C-2 and C-3 of its Man residues. Based on HPLC data (Table 2), the degree of *O*-acetylation of Man residues is 0.5. The intensities of the H-2 signals of 2-*O*-acetylated and 3-*O*-acetylated Man

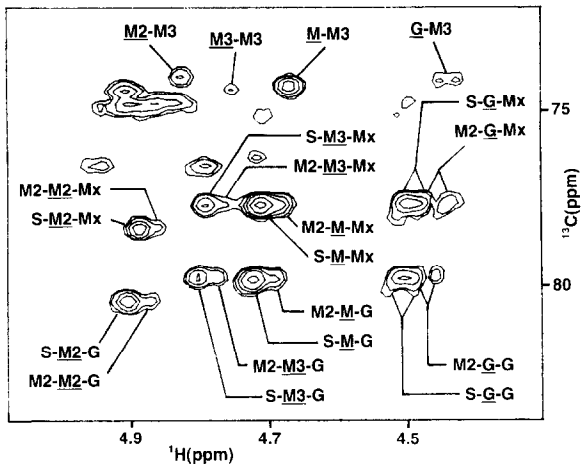

Fig. 4. Enlargement of the β-(1 → 4)-linkage region of the HMBC spectrum of fraction III. The following encoding is used: G, Glc; M, non-acetylated Man; M2, 2-*O*-acetylated Man; M3, 3-*O*-acetylated Man; Mx, M or M2; S, any monosaccharide, except M2. The cross-peaks are between H-1 of the underlined residue and C-4 of the residue at the right-hand side. For example: M2–M3–G refers to the cross-peak between H-1 of 3-*O*-acetylated Man and C-4 of Glc, whereby a 2-*O*-acetylated Man is attached to the 3-*O*-acetylated Man residue.

indicate that approximately 60% of the *O*-acetyl groups are found on the C-2 position of Man and 40% on the C-3 position of Man. No evidence was found for *O*-acetylated Glc residues. The proposed structure corresponds with those generally found in plant cell walls [7,17].

Water extract.—The monosaccharide composition of the water extract is given in Table 2. The extract is strongly enriched in Gal residues and, to a lesser extent, GalA, Rha and Ara. The ratio of GalA to Rha is 1.3. This composition suggests a pectic substance with a RG-I structure [17,24].

The ^{13}C NMR spectrum is given in Fig. 5. It shows 7 major signals at 105.66, 78.96, 75.81, 74.61, 73.12, 69.94 and 62.05 ppm, respectively. These signals correspond with those found by Davis et al. [4] for → 4)-β-D-Gal*p*-(1 → and the non-reducing end of

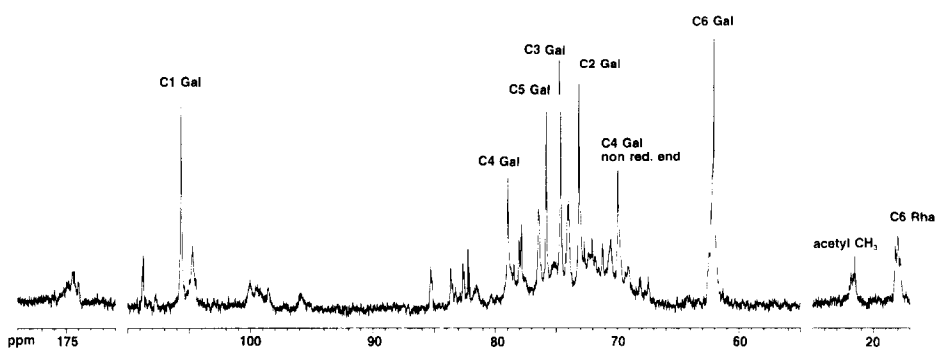

Fig. 5. ^{13}C NMR spectrum of the water extract.

Table 5
Assignment of ^{13}C and ^{1}H chemical shifts in ppm of the water extract, together with some reference data [4]

Residue		C-1/H-1	C-2/H-2	C-3/H-3	C-4/H-4	C-5/H-5	C-6/H-6
→ 4)-β-D-Gal *p*-(1 →	^{13}C	105.66	73.12	74.61	78.96	75.81	62.05
	^{1}H	4.60	3.67	3.81	4.14	3.75	3.78
→ 4)-β-D-Gal *p*-(1 → [a]	^{13}C	105.88	73.38	74.84	79.18	76.02	62.28
	^{1}H	4.68	3.72	3.81	4.21		
β-D-Gal *p*-(1 →	^{13}C	69.94					
	^{1}H	3.86					
β-D-Gal *p*-(1 → [a]	^{13}C	70.18					
	^{1}H	3.93					

[a] Reference data [4].

β-D-Gal *p*-(1 → (Table 5). It can thus be concluded that a β-(1 → 4)-linked galactan structure is present. The signals around 174, 22 and 18 ppm can be assigned to C=O of carbonyl groups (Ac, uronic acid), CH_3 of acetyl groups and C-6 of Rha residues, respectively. In the anomeric region several signals, other than the one at 105.66 ppm, can be found. The signal at 108.71 ppm arises from C-1 of α-L-Ara *f* residues [12,13,20], that at 104.72 ppm from C-1 of the Gal residue in β-D-Gal *p*-(1 → 4)-α-L-Rha *p*-(1 → [4], and those between 98.5 and 100.1 ppm can probably be attributed to C-1 of α-L-Rha *p* [15,25] and α-D-Gal *p*A [4]. The weaker signals between 67 and 85 ppm may arise from C-atoms of α-L-Ara *f* [12,13,20], α-L-Rha *p* [15,25] and α-D-Gal *p*A [4].

The ^{1}H NMR spectrum of the water extract confirms the presence of a β-(1 → 4)-linked galactan. All H atoms of → 4)-β-D-Gal *p*-(1 → and H-4 of the non-reducing Gal residue can be assigned (Table 5). Signals between 2.0 and 2.2 ppm indicate the presence of *O*-acetyl groups and those between 1.2 and 1.3 ppm the presence of Rha.

From these data an acetylated RG-I structure is likely, with a backbone consisting of α-L-Rha *p* and α-D-Gal *p*A residues, probably → 2)-α-L-Rha *p*-(1 → and → 4)-α-D-Gal *p*A-(1 → , which is generally found in pectic structures [7,17] and arabinogalactan side chains. The side chains mainly consist of a β-(1 → 4)-linked galactan and are attached by a Gal residue to Rha O-4. The signals from the Ara residues are too weak to deduce if they are present as branched or linear side chains.

In the ^{1}H NMR spectrum, chemical shifts for Rha H-6 were found both at 1.23 and 1.29 ppm, corresponding to 2-linked and 2,4-linked Rha, respectively [26]. The intensities of these two peaks show that approximately 35% of the Rha residues is 2-linked and 65% 2,4-linked, meaning that 65% of the Rha residues contains a side chain. This results in an average side chain length of 9 monosaccharide residues, which is generally found in RG-I pectic structures [17]. In RG-I structures the Ara residues tend to be located at the non-reducing end of the side chains [17]. Since there is a significant quantity of terminal non-reducing Gal present, not all side chains will contain Ara residues.

According to Fry [17] *O*-acetylation in RG-I normally occurs at C-2 or C-3 of GalA. If the acetyl groups are solely located on the GalA residues, the degree of *O*-acetylation of these residues will be 2, meaning they are fully acetylated.

The RG-I structure proposed is comparable to the pectic polysaccharide isolated by Davis et al. [4] from the EDTA extract of flax fibres. The difference is that their polysaccharide was depleted in Ara, which could be explained by a different extraction procedure. McDougall [6] found in the Me_2SO extract of flax fibres a RG-I type structure with a ratio of Ara to Rha of 1:1, which equals the Ara/Rha ratio in the hot-water extract.

Alkaline extracts.—Table 2 shows the monosaccharide composition of the precipitated and freeze-dried alkaline extracts. Both extracts are strongly enriched in Man and Glc, and the ratio of Man and Glc is 1.3 and 1.5 for the aq 5% and aq 17.5% NaOH extract, respectively. This approximates very closely the Man/Glc ratio of 1.5 of the Me_2SO fraction III. It is very likely that the alkaline extracts contain a glucomannan polysaccharide similar to that in the Me_2SO fraction III. The aq 5% NaOH extract contains an important quantity of Xyl residues, probable from a xylan structure similar to that in fraction II. The ratios of Gal, GalA and Rha are very similar in the water and alkaline extracts (1.0: 0.3: 0.2), suggesting that the alkaline extracts contain the same RG-I structure as the water extract.

It can thus be concluded that the alkaline extracts are composed of glucomannan, xylan and RG-I with structures similar to those found in the Me_2SO and water extract. Although identical in carbohydrate composition, these structures could probably not be extracted by Me_2SO or hot water due to steric hindrance by other cell-wall polysaccharides. Since alkali has a strong swelling effect on crystalline cellulose [27], it could facilitate the liberation of these polysaccharides. The difference between alkaline and other extracts is that the polysaccharides in the former are de-*O*-acetylated by the alkaline treatment.

Acknowledgements

The authors wish to thank the Directorate Science and Technology (DWT) of the Dutch Ministry of Agriculture, Nature Management and Fisheries for their financial support.

References

[1] R.H. Kirby, *Vegetable Fibres: Botany, Cultivation, and Utilization*, Leonard Hill Ltd., London, 1963, pp 15–45.
[2] C. Morvan, A. Jauneau, A. Flaman, J. Millet, and M. Demarty, *Carbohydr. Polym.*, 13 (1990) 149–163.
[3] C. Morvan, A. Abdul-Hafez, O. Morvan, A. Janeau, and M. Demarty, *Plant Physiol. Biochem.*, 27 (1989) 451–459.
[4] E.A. Davis, C. Derouet, C. Herve Du Penhoat, and C. Morvan, *Carbohydr. Res.*, 197 (1990) 205–215.
[5] D. Hourdet and G. Muller, *Carbohydr. Polym.*, 16 (1991) 409–432.
[6] G.J. McDougall, *Carbohydr. Res.*, 241 (1993) 227–236.
[7] A.M. Stephen, in G.O. Aspinall (Ed.), *The Polysaccharides*, Vol. 2, Academic Press Inc., London, 1983, pp 97–193.
[8] H.O. Bouveng and B. Lindberg, *Methods Carbohydr. Chem.*, 5 (1965) 147–150.
[9] K.A. Garleb, L.D. Bourquin, and G.C. Fahey, *J. Agric. Food Chem.*, 37 (1989) 1287–1293.

[10] R.J.A. Gosselink, J.E.G. van Dam, and F.H.A. Zomers, *J. Wood Chem. Technol.*, 15 (1995) 1–25.
[11] A. Bax, S.W. Sparks, and D.A. Torchia, *J. Am. Chem. Soc.*, 110 (1988) 7926–7927.
[12] R.A. Hoffmann, M. Roza, J. Maat, J.P. Kamerling, and J.F.G. Vliegenthart, *Carbohydr. Polym.*, 15 (1991) 415–430.
[13] R.A. Hoffmann, J.P. Kamerling, and J.F.G. Vliegenthart, *Carbohydr. Res.*, 226 (1992) 303–311.
[14] A. Bazus, L. Rigal, A. Gaset, T. Fontaine, J.M. Wieruszeski, and B. Fournet, *Carbohydr. Res.*, 243 (1993) 323–332.
[15] K. Bock, C. Pedersen, and H. Pedersen, *Adv. Carbohydr. Chem. Biochem.*, 42 (1984) 193–224.
[16] H.O. Kalinowski, S. Berger, and S. Braun, *^{13}C NMR Spektroskopie*, Thieme, Stuttgart–New York, 1984, pp 88–96.
[17] S.C. Fry, *The Growing Plant Cell Wall: Chemical and Metabolic Analysis*, Longman, Essex, 1988, pp 102–112.
[18] M. Kubackova, S. Karacsonyi, and L. Bilisics, *Carbohydr. Polym.*, 19 (1992) 125–129.
[19] F. Radjabi-Nassab, C. Ramiliarison, C. Monneret, and E. Vilkas, *Biochimie*, 66 (1984) 563–567.
[20] T. Watanabe, K. Inaba, A. Nakai, T. Mitsunaga, J. Ohnishi, and T. Koshijima, *Phytochem.*, 30 (1991) 1425–1429.
[21] R. Goldberg, L. Gillou, R. Prat, C. Herve Du Penhoat, and V. Michon, *Carbohydr. Res.*, 210 (1991) 263–276.
[22] P.-E. Jansson, L. Kenne, and E. Schweda, *J. Chem. Soc. Trans. I*, (1987) 377–383.
[23] E. Westerlund, R. Andersson, and P. Åman, *Carbohydr. Polym.*, 20 (1993) 115–123.
[24] M. McNeil, A.G. Darvill, and P. Albersheim, *Plant Physiol.*, 66 (1980) 1128–1134.
[25] J. Varljen, A. Lipták, and H. Wagner, *Phytochem.*, 28 (1989) 2379–2383.
[26] I.J. Colquhoun, G.A. de Ruiter, H.A. Schols, and A.G.J. Voragen, *Carbohydr. Res.*, 206 (1990) 131–144.
[27] E. Sjöström, *Wood Chemistry: Fundamentals and Applications*, 2nd ed., Academic Press Inc., London, 1993, pp 204–209.